

## Low-temperature structural phase transition in $\text{La}_2\text{NiO}_{4+\delta}$

Gerald Burns and F. H. Dacol

*IBM Research Division, Thomas J. Watson Research Center, Yorktown Heights, New York 10598-0218*

D. E. Rice and D. J. Buttrey

*Department of Chemical Engineering, Colburn Laboratory, University of Delaware, Newark, Delaware 19716*

M. K. Crawford

*E. I. du Pont de Nemours and Company, Wilmington, Delaware 19880-0356*

(Received 1 August 1990)

$\text{La}_2\text{NiO}_{4+\delta}$  ( $\delta=0$ ) has a high-temperature tetragonal (HTT) phase ( $T > 680$  K), a low-temperature orthorhombic (LTO) phase, and a low-temperature tetragonal (LTT) phase ( $T < 70$  K); that is,  $\text{HTT} \rightarrow \text{LTO} \rightarrow \text{LTT}$ . These phases are isomorphic to those of  $\text{La}_{2-x}\text{Ba}_x\text{CuO}_4$  ( $x=0.12$ ). Using Raman spectroscopy, we have measured the *c*-axis-polarized phonons. The  ${}^2A_{1g}$  modes of the HTT phase occur in all three phases at 155 and 445  $\text{cm}^{-1}$ , with energies and widths only weakly dependent upon temperature. The low-energy  $\text{NiO}_6$ -octahedra tilting modes (which drive the phase transitions) have been observed and clearly show the first-order nature of the  $\text{LTO} \rightarrow \text{LTT}$  phase transition. The lowest-energy Raman mode observed (at 70  $\text{cm}^{-1}$  with  $B_{1g}$  symmetry), allowed only in the LTT phase, involves rocking motion of the undisplaced in-plane oxygen atoms.

### INTRODUCTION

$\text{La}_2\text{NiO}_{4+\delta}$ , isostructural to the high-temperature superconductor  $\text{La}_2\text{CuO}_4$ , has the  $\text{K}_2\text{NiF}_4$  structure in its high-temperature tetragonal (HTT) form.<sup>1</sup> Near the stoichiometric limit ( $\delta \approx 0$ ), upon cooling,  $\text{La}_2\text{NiO}_4$  undergoes two structural phase transitions. Above room temperature, the structure transforms from the HTT phase to a lower-temperature orthorhombic (LTO) phase via a continuous second-order phase transition at a temperature,<sup>2,3</sup>  $T_{s1} = 680$  K. The second structural transition is from the LTO phase to a low-temperature tetragonal (LTT) phase at  $T_{s2} \approx 70$  K. Thus, with decreasing temperature, the phase transitions (and space groups) are

$$\begin{aligned} \text{HTT} \rightarrow \text{LTO} \rightarrow \text{LTT}, \\ \text{Tet.}(I4/mmm) \rightarrow \text{Ortho.}(Abma) \rightarrow \text{Tet.}(P4_2/ncm). \end{aligned} \quad (1a)$$

Both of the low-temperature structures have space groups that are subgroups of the high-temperature space group<sup>1,5</sup>

$$\begin{aligned} I4/mmm (D_{4h}^{17}) \rightarrow Abma (D_{2h}^{18}), \\ I4/mmm (D_{4h}^{17}) \rightarrow P4_2/ncm (D_{4h}^{16}). \end{aligned} \quad (1b)$$

However, the LTT space group is not a subgroup of the LTO space group so the  $\text{LTO} \rightarrow \text{LTT}$  phase transition is expected to be first order.

The  $\text{LTO} \rightarrow \text{LTT}$  transition in single-crystal  $\text{La}_2\text{NiO}_{4.00}$  has been investigated<sup>4</sup> using neutron scattering. A first-order transition ( $T_{s2} = 70.0$  K) is found, accompanied by a change of antiferromagnetic (AFM) spin structure. Single crystals of  $\text{La}_2\text{NiO}_{4.00}$  have also been studied using infrared (ir) spectroscopy<sup>6</sup> in the  $10 \leq T \leq 300$  K range. The first-order nature of the transition was confirmed by these studies, but no direct infor-

mation regarding the temperature dependence of the  $\text{NiO}_6$  octahedra tilting vibrations was obtained.

In this paper, we report polarized Raman spectroscopy results from single crystals of  $\text{La}_2\text{NiO}_{4+\delta}$  ( $\delta \approx 0$ ). In particular, we have measured the frequencies and symmetries of the Raman-active phonons in the LTO and LTT phases. These phases are characterized by tilts of the  $\text{NiO}_6$  octahedra about axes in the *ab* plane.<sup>1</sup> The  $\text{HTT} \rightarrow \text{LTO}$  transformation is driven by soft modes at the Brillouin-zone-boundary *X* point in the HTT phase. The  $\text{LTO} \rightarrow \text{LTT}$  transition causes the *Z* point in the LTO phase to fold over to the zone center in the LTT phase. By symmetry, the latter transition cannot be second order. In the LTO and LTT phases, the octahedra vibrate (rock) about their newly displaced positions. These modes are Brillouin-zone center, Raman-active modes of  $A_g$  symmetry in the LTO phase and  $A_{1g} + B_{1g}$  symmetry in the LTT phase.

### EXPERIMENT

Because of the sensitive dependence of structure on oxygen stoichiometry, it is essential to work with well-characterized samples. For example, the  $\text{LTO} \rightarrow \text{LTT}$  phase transition is not observed for crystals with large  $\delta$  value.<sup>7</sup> Our single crystals were grown by radio-frequency-induction skull melting from starting materials of 99.997% or better nominal purity. This is a cold-crucible technique, so contamination during crystal growth is avoided. Details are described elsewhere.<sup>8</sup> Selected crystals were oriented by Laue back diffraction, cut, and polished. They were subsequently annealed isothermally at 1270 K in a  $\text{CO-CO}_2$  buffer which fixed the equilibrium oxygen fugacity ( $\log_{10} f_{\text{O}_2} = -11.55 \pm 0.03$ ). After a 4-h anneal, the crystals were quenched to room

temperature.

The HTT structure of  $\text{La}_2\text{NiO}_{4+\delta}$  ( $\delta=0.00$ ) is shown in Fig. 1(a). Instead of the usual body-centered tetragonal (bct) unit cell ( $I4/mmm$ ) with two formula units ( $Z=2$ ), an equivalent<sup>1,5</sup> face-centered tetragonal (fct) unit cell is shown with  $Z=4$ . The **a** and **b** axes of the fct cell are rotated by  $45^\circ$  and are  $\sqrt{2}$  longer than those of the bct cell. Also, the crystallographic space-group notation is  $F4/mmm$  for the fct cell rather than  $I4/mmm$ , for the bct cell, but since they are merely different cells for the same structure, the Schoenflies symbol ( $D_{4h}^{17}$ ) is the same.<sup>1</sup>

The LTO structure [Fig. 1(b)] is obtained by rotating the  $\text{NiO}_6$  octahedra about the [010] axis such that the rotation direction alternates between nearest neighbors in the basal plane, as required by corner sharing of the  $\text{NiO}_6$  octahedra. Thus, in the (001) planes, neighboring octahedra are contrarotated. However, in the (010) planes, neighboring octahedra are corotated [Fig. 1(b)]. The atomic displacements of the oxygen atoms in the Ni-O planes can be written as

$$U_{96} = u_{14z} + u_{15z} - u_{24z} - u_{25z} - u_{34z} - u_{35z} + u_{44z} + u_{45z} \quad (2a)$$

following Geick and Strobel<sup>9</sup> where the atoms are numbered as in Fig. 1(a). The apical oxygen atoms  $\text{O}(z)$  and La atoms, along the *c* axis above and below the Ni atoms, displace in the *xy* direction as would be expected<sup>9</sup> for rigid  $\text{NiO}_6$  octahedra. However, for clarity, the displacement vectors for La and  $\text{O}(z)$  atoms are not shown. In the LTO structure the rotation about the corner atom (11) and the *A* face-centered atom (41) is the same, but this rotation is opposite to that of the other two face-centered atoms (21 and 31). Thus, the space group is *A* centered. If the **a** and **b** axes are interchanged,<sup>1</sup> the resulting space group is  $Bmab$  ( $D_{2h}^{18}$ ).

The LTT structure is shown in Fig. 1(c). The displacements are obtained by rotating the  $\text{NiO}_6$  octahedra about  $\langle 110 \rangle$  directions such that in the basal plane nearest

neighbors are contrarotated, as required by corner sharing of the  $\text{NiO}_6$  octahedra. Along the *c* axis the rotation axis alternates between  $[110]$  and  $[\bar{1}\bar{1}0]$ . The resulting in-plane oxygen atom displacements can be written as<sup>9</sup>

$$U_{95} + U_{96} = u_{14z} + u_{15z} - u_{24z} - u_{25z}, \quad (2b)$$

which leaves half of the basal plane oxygen atoms undisplaced.

The HTT structure [Fig. 1(a)] has an *X*-point Brillouin-zone boundary vibration whose motion is similar to the displacements shown in Fig. 1(b). In the HTT phase, with decreasing temperature, these vibrations become soft, with their frequency approaching zero, triggering a phase transition to the LTO phase. For isostructural HTT  $\text{La}_2\text{CuO}_4$ , these soft zone boundary, *X*-point phonons have been observed by inelastic neutron scattering.<sup>10</sup> In the LTO phase, the tilted octahedra [Fig. 1(b)] continue to vibrate (rock) with a similar motion. However, this vibration is a zone-center, Raman-active<sup>11,12</sup>  $A_g$  mode (point group  $mmm - D_{2h}$ ). This  $A_g$  mode becomes soft, approaching zero frequency, as the LTO  $\rightarrow$  HTT phase transition is approached with increasing temperature.

The HTT and LTT structures are similarly related by octahedra tilts, although a direct HTT  $\rightarrow$  LTT phase transition has not yet been observed. In the LTT phase, the tilted octahedra<sup>13</sup> [Fig. 1(c)] vibrate (rock) in a zone center Raman-active  $A_{1g}$  mode, which involves only the tilted, out-of-plane oxygen atoms. Furthermore, a second zone-center, octahedral rocking motion becomes  $B_{1g}$  Raman active. This vibration is described by the following motion of the in-plane oxygen atoms:

$$U_{95} - U_{96} = \pm (v_{34z} + v_{35z} - v_{44z} - v_{45z}), \quad (2c)$$

where the atoms are numbered as in Fig. 1(a). Note the resemblance between this  $B_{1g}$  vibration, which occurs about *undisplaced* oxygen positions, and the  $A_{1g}$  vibration described above which occurs about *displaced* oxygen positions. We can use the polarized Raman selection rules to separate these modes.

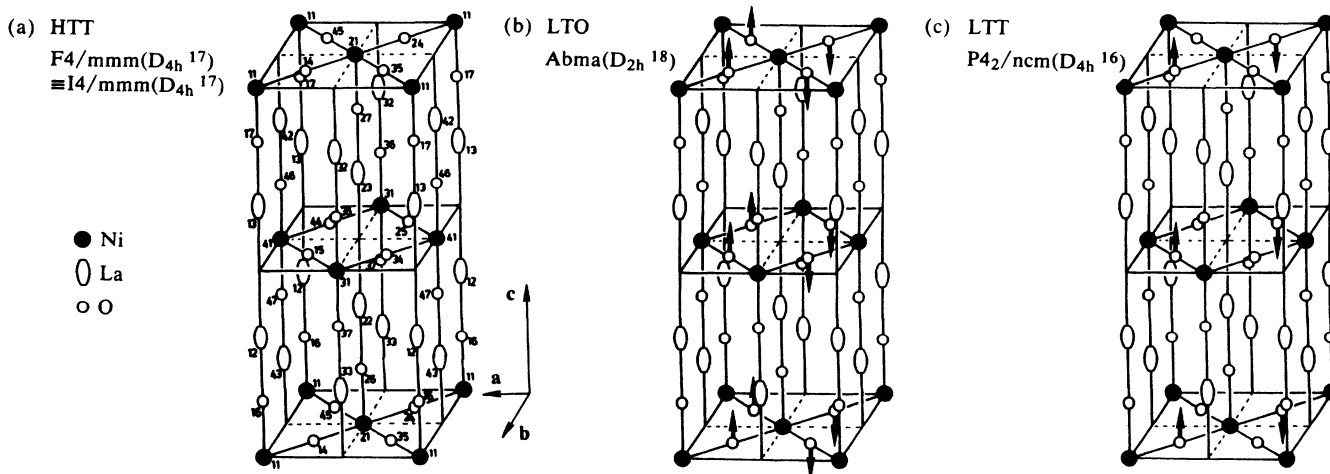


FIG. 1. (a) The undistorted high-temperature tetragonal (HTT) structure. The numbers label the atoms (Ref. 9). (b) and (c) The oxygen displacements for the Ni-O plane are shown in the low-temperature orthorhombic (LTO) and low-temperature tetragonal (LTT) structures, respectively. The apical oxygen and La atoms are also displaced, but these displacements are omitted for clarity.

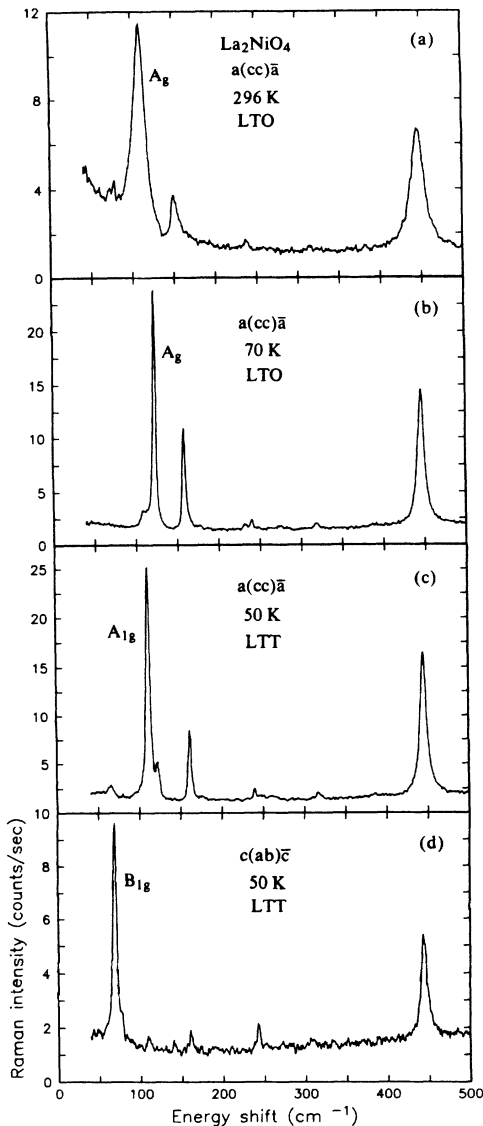


FIG. 2. (a) and (b) The  $A_g$  modes in the HTT phase, at room temperature and at 70 K (just above the phase transition), respectively. (c) The same but just below the phase transition, in the LTT phase. (d) The  $B_{1g}$  spectrum in the LTT phase.

## RESULTS

Experimental  $A_g$  and  $A_{1g}$  Raman results are shown in Figs. 2(a)–2(c) at various temperatures. The phonons near 155 and 455  $\text{cm}^{-1}$  correspond to the  ${}^2A_{1g}$  modes allowed in the HTT phase,<sup>11,12</sup> these vibrations are relatively temperature independent and their low-temperature frequencies are listed in Table I. On the other hand, the mode at 123  $\text{cm}^{-1}$  at 70 K [Fig. 2(b)] shifts to 110  $\text{cm}^{-1}$  at 296 K [Fig. 2(a)] and continues to decrease in frequency as the temperature is further raised.<sup>14</sup> We assign it to the soft vibration, connecting the tilted octahedra in the LTO phase to the untilted octahedra in the HTT phase [Eq. (1)]. This mode has also been observed<sup>11,12</sup> in the LTO phase of  $\text{La}_2\text{CuO}_4$ .

Figures 2(b) and 2(c) show the 123- $\text{cm}^{-1}$  vibration in the LTO phase and the 110- $\text{cm}^{-1}$  mode in the LTT phase (Table I). These two modes are also seen in Fig. 3, where the first-order nature of the phase transition is clear. The shift from 123 to 110  $\text{cm}^{-1}$  is discontinuous, as expected, for a first-order phase transition.

The LTT cross-polarized spectrum is shown in Fig. 2(d).  $B_{1g}$  modes are allowed in this polarization and a strong mode at 70  $\text{cm}^{-1}$  is observed. The weaker features at 110, 155, and 455  $\text{cm}^{-1}$  are due to polarization leakage from the  $A_g$  modes.

## DISCUSSION

The different symmetry adapted vectors for the  $A_g$  and  $A_{1g}$  modes in the LTO and LTT phases lead to surprisingly small changes in the energies of these phonons (Table I). Since fewer Ni-O bonds bend in the LTT  $A_{1g}$  vibration, the lower frequency for this mode is reasonable.

As the temperature increases from 10 to 50 K in the LTT phase, the  $B_{1g}$  mode softens by about 4  $\text{cm}^{-1}$  before folding back to the  $Z$  point in the LTO phase. This temperature dependence demonstrates the first-order nature of the LTT-LTO phase transition. The behavior of the  $A_g$  and  $A_{1g}$  phonons through the LTO  $\rightarrow$  LTT phase transition (Fig. 3) also clearly demonstrates the first-order nature of the phase transition. These Raman results are in excellent agreement with ir results<sup>6</sup> and structural neutron studies.<sup>4</sup>

In the LTT phase, a surprising result of this work is the

TABLE I.  $\text{La}_2\text{NiO}_4$  Raman active phonon symmetries ( $S$ ), energies ( $\text{cm}^{-1}$ ), and assignments in LTO and LTT phases. All modes involve atomic vibration parallel to the  $c$  axis.

LTO ( $T=70$ K)			LTT ( $T=50$ K)		
$S$	Energy	Assignment	$S$	Energy	Assignment
$A_g$	445	O( $z$ )	$A_{1g}$	445	O( $z$ )
$A_g$	155	La	$A_{1g}$	155	La
$A_g^a$	123	NiO <sub>6</sub> rotation about displaced positions	$A_g^a$	110	NiO <sub>6</sub> rotation about displaced positions
			$B_{1g}^a$	70	NiO <sub>6</sub> rotation about undisplaced positions

<sup>a</sup>Note that the LTO zone-center  $A_g$  mode combines with the LTO  $Z_3^+$  Brillouin-zone boundary mode to become the  $A_{1g}$  and  $B_{1g}$  zone-center modes in the LTT phase.

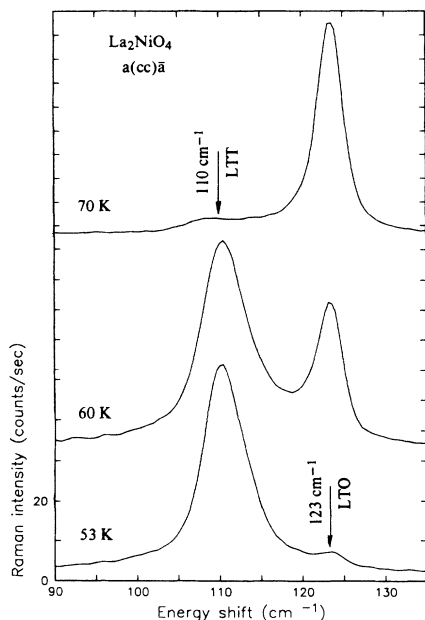


FIG. 3. The  $a(cc)\bar{a}$  Raman spectra showing the first-order LTO $\rightarrow$ LTT phase transition. The  $A_{1g}$  mode at  $110\text{ cm}^{-1}$  in the LTT phase and the  $A_{1g}$  mode at  $123\text{ cm}^{-1}$  in the LTO phase are both apparent. Note in this, and the preceding figure, the raw data are presented.

observation of a sharp, low-energy  $B_{1g}$  mode at  $\approx 70\text{ cm}^{-1}$  [Table I and Fig. 2(d)]. This mode has a considerably lower frequency than that of the  $A_{1g}$  rocking mode ( $110\text{ cm}^{-1}$ ). We can understand the low energy of the  $B_{1g}$  mode in the following manner. After a soft mode triggers a phase transition, then with decreasing temperature, the frequency of this mode increases (hardens). The vibrational pattern [Eq. (2c)] of the  $B_{1g}$  mode is similar to that of the displacement (and vibrational) pattern of the  $A_{1g}$  mode [Fig. 1(c)]. However, for the  $B_{1g}$  mode, the vibration is about *undisplaced* oxygen positions while for the  $A_{1g}$  mode, the vibration is about *displaced* oxygen positions. Thus, the  $A_{1g}$  mode is effectively hardened while this is not the case for the  $B_{1g}$  mode.

The mechanisms for the LTO $\rightarrow$ LTT structural transformation has been studied<sup>15,16</sup> in  $(\text{CH}_3\text{NH}_3)_2\text{MCl}_4$ , where  $M = \text{Mn, Cd}$ , and evidence was presented for an in-

termediate orthorhombic phase (space group  $Pccn$  ( $D_{2h}^{10}$ )) which could form, via a second-order transition, from either the LTT structure or the LTO structure. Our Raman results on  $\text{La}_2\text{NiO}_4$  present a different picture of the phase transition, possibly due to the lack of a complex organic cation in the structure. Based on our Raman data, there is no need to involve an intermediate  $Pccn$  phase since the  $B_{1g}$  Raman mode, which is a direct measure of the order parameter for LTT-LTO transition, softens only slightly upon approaching the transformation temperature.

Finally, we discuss the relevance of our Raman results in  $\text{La}_2\text{NiO}_4$  to the  $\text{La}_{2-x}\text{Ba}_x\text{CuO}_4$  system. There, for  $x \sim 0.12$ , the LTO $\rightarrow$ LTT phase transition occurs<sup>13</sup> near 60 K, leading to an apparently nonsuperconducting LTT phase. This transition has been described as the result of the softening to zero energy with temperature of the second HTT  $X$ -point phonon. There is, however, no experimental data on this phonon in  $\text{La}_{2-x}\text{Ba}_x\text{CuO}_4$  near the LTO $\rightarrow$ LTT phase transition. Thus, our Raman data in  $\text{La}_2\text{NiO}_4$  furnish evidence that this mode does *not* soften significantly at the LTT-LTO structural transformation. Based upon the similar lattice dynamics expected for  $\text{La}_2\text{NiO}_4$  and  $\text{La}_2\text{CuO}_4$ , we would expect the  $B_{1g}$  mode in  $\text{La}_{1.88}\text{Ba}_{0.12}\text{CuO}_4$  to behave in an analogous manner. If, however, the LTO-LTT phase transition is strongly coupled to the charge carriers in  $\text{La}_{2-x}\text{Ba}_x\text{CuO}_4$ , the situation there may differ from our observations in insulating  $\text{La}_2\text{NiO}_4$ .

In conclusion, we have reported Raman measurements of modes involving  $c$ -axis motion of atoms in  $\text{La}_2\text{NiO}_4$  in the LTO and LTT phases and through the structural transformation. These measurements demonstrate the first-order nature of this transformation and, in addition, provide the first clear picture of the soft phonon dynamics associated with this phase transition in these layered materials.

#### ACKNOWLEDGMENTS

It is a pleasure to thank L. Lardear for help with single-crystal orientation. Work at the University of Delaware was supported by the National Science Foundation under Contract No. DMR-8914080.

<sup>1</sup>G. Burns and A. M. Glazer, *Space Groups for Solid State Scientists* (Academic, New York, 1990), Chaps. 7 and 9, and Appendix 9.

<sup>2</sup>J. M. Honig and D. J. Buttrey, in *Localization and Metal Insulator Transitions*, edited by H. Fritzche and D. Adler (Plenum, New York, 1985), p. 409.

<sup>3</sup>C. P. Tavares, *Mater. Res. Bull.* **20**, 972 (1985).

<sup>4</sup>G. H. Lander *et al.*, *Phys. Rev. B* **40**, 4463 (1989).

<sup>5</sup>*International Tables for Crystallography*, edited by T. Hahn (Reidel, Dordrecht, 1987), Vol. A.

<sup>6</sup>D. E. Rice *et al.*, *Phys. Rev. B* **42**, 8787 (1990).

<sup>7</sup>T. Freltoft *et al.*, *Phys. Rev. B* (to be published).

<sup>8</sup>D. J. Buttrey *et al.*, *J. Solid State Chem.* **54**, 407 (1984).

<sup>9</sup>R. Geick and K. Strobel, *J. Phys. C* **10**, 4221 (1977).

<sup>10</sup>R. J. Birgeneau *et al.*, *Phys. Rev. Lett.* **59**, 1329 (1987); *Phys. Rev. B* **38**, 185 (1988); **39**, 4327 (1989).

<sup>11</sup>G. Burns *et al.*, *Solid State Commun.* **68**, 67 (1988).

<sup>12</sup>W. H. Weber *et al.*, *Solid State Commun.* **68**, 61 (1988).

<sup>13</sup>J. D. Axe *et al.*, *IBM J. Res. Dev.* **33**, 382 (1989); *Phys. Rev. Lett.* **62**, 275 (1989).

<sup>14</sup>We have heated another crystal above room temperature and observed that the frequency of this mode decreases substantially while the  $155$  and  $445\text{ cm}^{-1}$  modes have very little temperature dependence.

<sup>15</sup>M. Couzi, A. Daoud, and R. Perret, *Phys. Status Solidi* **41**, 271 (1977).

<sup>16</sup>T. Gyto *et al.*, *Phys. Rev. B* **22**, 3452 (1980).